ORIGINAL ARTICLE

Shipborne gravimetry in the Baltic Sea: data processing strategies, crucial findings and preliminary geoid determination tests

Biao Lu[1,2,3] · Franz Barthelmes[2] · Min Li[2,3] · Christoph Förste[2] · Elmas Sinem Ince[2] · Svetozar Petrovic[2] · Frank Flechtner[2,3] · Joachim Schwabe[4] · Zhicai Luo[5,6] · Bo Zhong[1,7] · Kaifei He[8]

Abstract

Shipborne gravimetry is an essential method to measure the Earth's gravity field in the coastal and offshore areas. It has the special advantages of high-accuracy and high-resolution measurements in coastal areas compared to other techniques (e.g., satellite gravimetry, airborne gravimetry, and altimetry) used to obtain information about the gravity field. In this paper, we present the data processing strategies of shipborne gravimetry in GFZ. One key point is that the most suitable filter parameters to eliminate disturbing accelerations are determined by studying the GNSS-derived kinematic vertical accelerations and the measurement differences at crossover points. Apart from that, two crucial issues impacting on shipborne gravimetry are the seiches in some harbors and the squat effect in the shallow water. We identified that inclusion of GNSS-derived kinematic vertical accelerations can help to improve the shipborne gravimetry results at these special cases in the Baltic Sea. In the absence of the GNSS-derived vertical accelerations, the cutoff wavelength of the low-pass filter should be large enough to filter out these disturbing acceleration signals which causes a coarser spatial resolution of the gravity measurements. Therefore, the GNSS-derived kinematic vertical accelerations are very useful for optimum shipborne gravimetry. Finally, our shipborne gravimetry measurements are successfully used to verify the previous gravimetry data and improve the current geoid models in the Baltic Sea.

Keywords Shipborne gravimetry · Chekan-AM · GNSS · FAMOS project · Baltic Sea

✉ Biao Lu
   biaolu@gfz-potsdam.de

   Franz Barthelmes
   bar@gfz-potsdam.de

   Min Li
   minli@gfz-potsdam.de

   Christoph Förste
   foer@gfz-potsdam.de

   Elmas Sinem Ince
   elmas.sinem.ince@gfz-potsdam.de

   Svetozar Petrovic
   sp@gfz-potsdam.de

   Frank Flechtner
   flechtne@gfz-potsdam.de

   Joachim Schwabe
   Joachim.Schwabe@bkg.bund.de

   Zhicai Luo
   zcluo@hust.edu.cn

   Bo Zhong
   bzhong@sgg.whu.edu.cn

   Kaifei He
   kfhe@upc.edu.cn

[1] School of Geodesy and Geomatics, Wuhan University, Wuhan 430079, People's Republic of China

[2] GFZ German Research Centre for Geosciences, Telegrafenberg, 14473 Potsdam, Germany

[3] Department of Geodesy and Geoinformation Science, Technical University of Berlin, 10623 Berlin, Germany

[4] Federal Agency for Cartography and Geodesy, 04105 Leipzig, Germany

[5] MOE Key Laboratory of Fundamental Physical Quantities Measurement, School of Physics, Huazhong University of Science and Technology, Wuhan 430074, People's Republic of China

[6] Institute of Geophysics, Huazhong University of Science and Technology, Wuhan 430074, People's Republic of China

[7] Key Laboratory of Geospace Environment and Geodesy, Ministry of Education, Wuhan University, Wuhan 430079, People's Republic of China

1 Introduction

Since 2013, German Research Centre for Geosciences (GFZ) has performed five shipborne gravimetry missions over the Baltic Sea. Four particular campaigns were carried out in cooperation with the German Federal Agency for Cartography and Geodesy (BKG) and the Federal Maritime and Hydrographic Agency (BSH) with the aim to measure gravity values on the Baltic Sea in order to improve the local geoid. The BKG is responsible for the national German quasigeoid model, whereas the BSH provided the survey vessels. A part of the activities is linked to the ongoing project "Finalising Surveys for the Baltic Motorways of the Sea" (FAMOS), led by the Swedish Maritime Administration and co-financed by the European Union. The main purpose of the FAMOS project is hydrographic surveying of the Baltic Sea to support sustainable and safe shipping. It contributes to Blue Growth which is the long-term strategy to support sustainable growth in the marine and maritime sectors as a whole in this region. One of the activities in this project is shipborne gravimetry to obtain high-quality gravity measurements to verify and check the quality of the existing gravity data, as well as to fill data gaps in this region. Finally, a high-quality geoid model will be developed based on existing and new gravity data which will be used as a future-proof geodetic chart datum in the entire Baltic Sea.

The platforms used for shipborne gravimetry in the Baltic Sea are the research vessels AIRISTO (in 2015), CAPELLA (in 2013), DENEB (in 2015 and 2016) and JACOB HÄGG (in 2016). An example of these research vessels is shown in Fig. 1a. The gravimetry equipment Chekan-AM is a mobile air–marine gravimetric system which is developed by CSRI Elektropribor (Blazhnov 2002) (Fig. 1b). This kind of integrated mobile gravimetric system has already been used on various platforms in many different projects, and there are many operational experiences gained by different teams (e.g., Zheleznyak 2010; Krasnov et al. 2011, 2014; Zheleznyak et al. 2015; Petrovic et al. 2016).

In principle, the raw measurements from a mobile gravimeter (Chekan-AM or other gravimeters) contain not only gravity signals, but also all other kinematic vertical accelerations including high-frequency accelerations which can be treated as disturbing noise. According to recent studies (e.g., Blazhnov 2002; Krasnov et al. 2011; Sokolov 2011; Krasnov and Sokolov 2015) and the operation manual of the gravimeter Chekan-AM, shipborne gravimetry does not need to consider these external vertical accelerations (e.g., GNSS-derived kinematic vertical accelerations). They argued that the basic period of these disturbing accelerations is within

6–10 s and can be effectively suppressed by a smoothing filter. Therefore, shipborne gravimetry measurements are usually not corrected for these disturbances. However, the Chekan-AM measurements were exposed also to disturbing accelerations with longer periods in the same range as the expected gravity signal in some harbors of the Baltic Sea. For geoid improvement, the absolute reference of the gravity is of particular interest (in contrast to, e.g., exploration geophysics, where relative accuracy, or precision, is sufficient). Therefore, a constant drift behavior of the gravimeter and also the reference readings in the harbor are important for this application. In this context, the disturbing accelerations with longer periods (seiches) in the harbor are interesting, because they might affect the harbor tie. For example, the Chekan-AM measurements in the harbor Trelleborg still contain oscillation signals (several mGal) after passing a low-pass filter with a cutoff wavelength of 200 s. One simple solution is to apply a stronger smoothing filter to filter these oscillation signals out. However, considering the existence of disturbing accelerations with longer periods (e.g., seiches) in the open sea, this reduces the spatial resolution of the measurements. Fortunately, we find that these oscillation signals (seiches) in the harbors can also be eliminated by subtracting the GNSS-derived kinematic vertical accelerations from Chekan-AM measurements which is presented in this article.

The Chekan-AM measurements could also contain disturbing accelerations of longer periods (longer than the basic period of 6–10 s) which cannot be ignored in the open sea. However, GNSS-derived kinematic vertical accelerations of longer wavelengths are, since derived from measurements, not error-free either. Hence, their contribution to an improvement depends on signal-to-noise ratio. In such cases, we analyze the spectrum of Chekan-AM measurements and that of GNSS-derived kinematic vertical accelerations to find a suitable range of the cutoff wavelength of the low-pass filter to suppress these disturbing acceleration signals. Additionally, the statistics of gravity differences at the crossover points of measured tracks help us to determine the most suitable parameters for the low-pass filter.

From our investigations, we also find that the measurements from Chekan-AM contain sudden changes of several mGal when the research vessel moves across sea channels in shallow water. The depth of such channels is typically about 11 m, which is 5 m deeper than the normal seafloor according to the bathymetry measurements. It can be shown that these sudden changes in the gravity measurements are not caused by the gravitational attraction of the density contrast, but by the vertical movement of the moving platform due to the squat effect. The squat is the vertical downward movement of a vessel in case of increasing speed or/and decreasing water depth beneath the vessel. The physical reason is the increasing relative speed of the water between ground and vessel and the resulting Bernoulli effect (e.g., Bernoulli 1968; Hàrting et al.

[8]   School of Geosciences, China University of Petroleum, Qingdao 266580, People's Republic of China
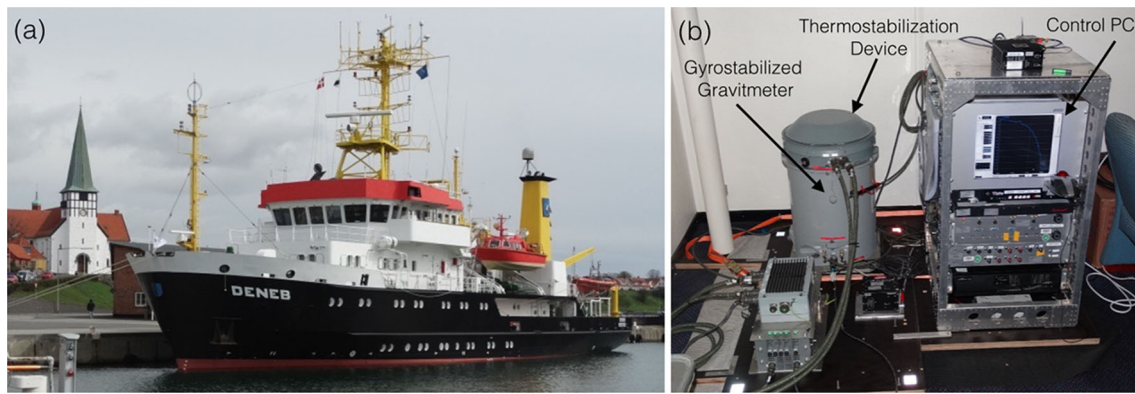
Fig. 1 **a** An example of research vessels: DENEB. **b** The mobile air–sea gravimeter: Chekan-AM

2004; Varyani 2006; Jachowski 2008). One simple method to deal with this problem is to remove these parts of measurements while another method is to apply a stronger smoothing filter which reduces the spatial resolution of the gravity measurements. According to our research, the change of several mGal will be smoother or even eliminated after subtracting the GNSS-derived kinematic vertical accelerations.

In this article, we focus on the data processing strategy of shipborne gravimetry to get high-accuracy and high-resolution gravimetry measurements in the Baltic Sea. In particular, the use of GNSS-derived kinematic vertical accelerations is investigated to improve the quality of the gravity data. In Sect. 2, the basic data processing strategy is presented briefly. In Sect. 3, numerical results of the crucial findings, the key question to find suitable parameters for the FFT low-pass filter and preliminary tests in geoid determination are given. In Sect. 4, our current findings of shipborne gravimetry in the Baltic Sea are summarized.

2 Data processing strategy of shipborne gravimetry

2.1 Processing of gravimeter recordings

The gravity sensor of Chekan-AM is designed as a double quartz elastic system (two quartz torsion fibers) to measure accelerations along the direction of the sensitive axis. The system is placed in a viscous liquid to damp high-frequency accelerations (vibrations). To keep the sensitive axis of this sensor in the vertical direction, it is mounted on a GNSS-supported gyro-stabilized platform (Sokolov 2011). The equation to calculate the gravity value from Chekan-AM raw measurements is:

$$g = g_{Chekan} - a_{GNSS} + \delta g_{Etvs} - \delta g_{HAC} - \delta g_{drift} + \delta g_{link} \quad (1)$$

where g_{Chekan} is the raw gravity measurement from the Chekan-AM gravimeter, a_{GNSS} is the GNSS-derived kinematic vertical acceleration of the moving platform. Here, the minus sign between g_{Chekan} and a_{GNSS} means that the vertical (up) acceleration from GNSS has the same definition as gravity (positive in the downward direction). δg_{Etvs} is the *Eötvös* correction (e.g., Harlan 1968; Jekeli 2001), δg_{HAC} is the horizontal acceleration correction as the vertical acceleration is also influenced by horizontal components, δg_{drift} is the instrumental drift correction, δg_{link} is the difference between the reference gravity value and the measurement of Chekan-AM at the base station. A more detailed processing scheme of shipborne gravimetry with the gravimeter Chekan-AM can be found in the operation manual of Chekan-AM and has been also presented by Krasnov et al. (2011) and Krasnov and Sokolov (2015). They also mentioned that it is not necessary to take into account the external vertical acceleration for shipborne gravimetry. However, we use external vertical accelerations (GNSS-derived kinematic vertical accelerations) to find the suitable parameters of the low-pass filter and investigate the special cases during shipborne gravimetry missions in the Baltic Sea.

2.2 Determination of the GNSS kinematic trajectories and accelerations

The GNSS kinematic trajectories are computed based on Differential GPS (DGPS) method (He 2015; Li et al. 2018). Here, carrier phase observations are used in DGPS method. It has been already proved that an accuracy of 1–2 cm in the horizontal and 1–5 cm in the vertical directions can be obtained with DGPS by applying multi-GNSS systems (GPS and GLONASS). Additionally, by using the a priori distance constraints and a common atmospheric delay parameter estimation strategy on multiple kinematic stations, the accuracies of the estimated kinematic state parameters can be further improved, especially in the vertical direction (the improvement of several mm) (He et al. 2016). Furthermore, we also
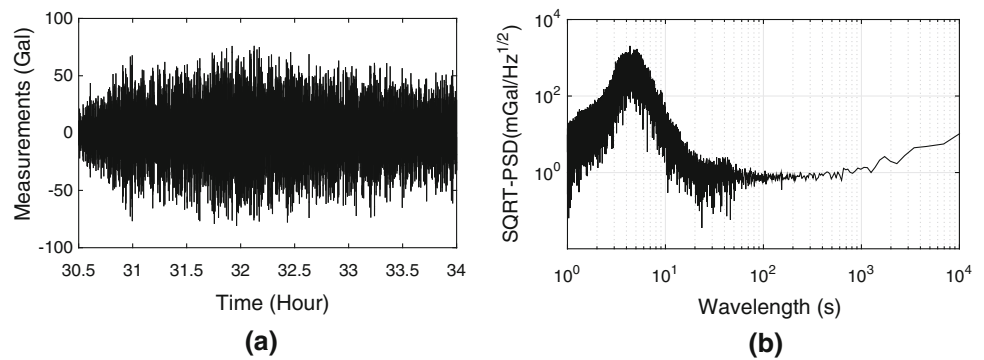
checked the sea surface height (calculated from GNSS) differences at crossover points. For example, the RMS of height differences at the crossover points (50 points) is 8.8 cm (with the largest difference of 13.4 cm) from the shipborne gravimetry mission "Deneb 2016". The corresponding accuracy (standard deviation of a single measurement) in the vertical direction is about $8.8/\sqrt{2} \approx 6.2$ cm according to the law of error propagation. Since the vertical gravity gradient is about 0.3086 mGal/m and the required accuracy of shipborne gravimetry is sub-mGal, the GNSS-based kinematic positioning is sufficient for determination of the trajectory of the research vessel.

For the determination of the kinematic vertical accelerations, we use derivatives of the kinematic velocities with respect to time in the vertical direction. The kinematic velocity of the research vessel is calculated based on the L1 carrier phase observations due to the lower noise. The GNSS-based double-differencing (DD) observation equation for velocity determination is as follows (Cannon et al. 1997; Bruton et al. 1999; He 2015):

$$-e_k^{p,q} V_k = \nabla \Delta \dot{\varphi}_{k,r}^{p,q} - e_{k,r}^p V^p + e_{k,r}^q V^q + \nabla \Delta \dot{u}_{k,r}^{p,q} \qquad (2)$$

where p, q are common satellites observed by a kinematic station k and a reference station r; e is the unit vector of the satellite and receiver at the direction cosine; V is the velocity vector; $\nabla \Delta$ means the DD operator; a dot represents the first derivative with respect to time; $\varphi_{k,r}^{p,q}$ denotes the double differenced carrier phase derived Doppler measurements; $\dot{u}_{k,r}^{p,q}$ denotes the modeling error and measurement error rates for carrier phase observations.

In DD processing, most error sources such as ionosphere, troposphere, tide and multipath effects can be significantly eliminated, so only the satellite orbit error remains to be taken into account. According to the IGS reports, Ultra-Rapid orbits can even achieve an accuracy of about 5 cm, which is sufficient for obtaining velocity estimates at the mm/s level (Serrano et al. 2004). Thus the IGS Final orbits, also the Rapid and Ultra-Rapid products can be used. Equation 2 can be directly solved by the classical least-squares adjust-

ment when more than four GNSS satellites are observed. This method had already been successfully used in airborne gravimetry for the determination of the GNSS-derived kinematic vertical accelerations (Lu et al. 2017).

2.3 The low-pass filter

The gravity variations in the Baltic Sea are expected to be several tens of mGal. However, the range of the raw shipborne gravimetry measurements extends to several tens of Gal for a typical track (see Fig. 2a) because of the other kinematic vertical accelerations (treated as noise). Fortunately, these disturbing signals in Chekan-AM raw measurements are mainly concentrated in the high frequencies, as shown in Fig. 2b, and they can be removed by applying an appropriate low-pass filter. Apart from that, GNSS-derived kinematic vertical accelerations used to detect the ship's vertical movements are not accurate enough in high-frequency parts to be considered to correct the gravimetry measurements. Therefore, a low-pass filter needs to be applied to both Chekan-AM measurements and GNSS-derived kinematic vertical accelerations to filter out the noisy components. In our study, a fast Fourier transform (FFT) filter is used as a low-pass filter which was effectively applied in airborne gravimetry (Childers et al. 1999; Lu et al. 2017). The main advantage is that the FFT filter, which is characterized by the cutoff wavelength, the transition region (sharpness or steepness of cutoff) and the shape of the transfer function (we use a cosine type in our study), can be simply defined directly in the frequency domain, as shown in Fig. 3. The main parameter of the FFT low-pass filter is the cutoff wavelength as it corresponds to the resolution of the final gravimetry results. The other one is the length of the transition zone which is related to the oscillations of the unit impulse response of the low-pass filter (Akaike 1968; Rabiner and Gold 1975). The length of the transition zone should not be designed too short. In other words, the oscillations of the unit impulse response should be designed not very large. A practical method to choose the cutoff wavelength and the length of the transition zone is given in Sect. 3.2.
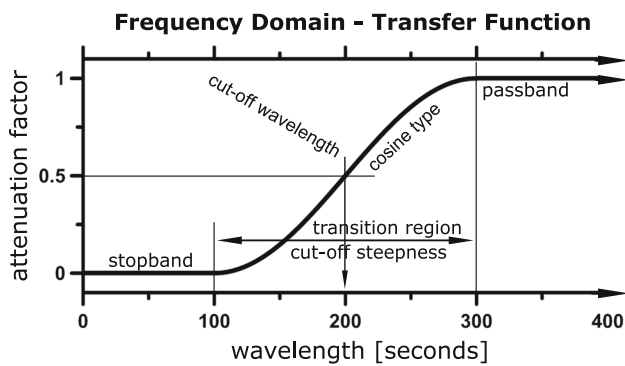
Fig. 3 Transfer function of the low-pass filter in the frequency domain

3 Analysis and numerical results

Five shipborne gravimetry campaigns have been carried out in the Baltic Sea by GFZ since 2013. The root-mean-square (RMS) of the gravity differences at crossover points is 0.76 mGal (380 crossover points). The corresponding accuracy (standard deviation of a single measurement) of these campaigns is about $0.76/\sqrt{2} \approx 0.5$ mGal according to the law of error propagation. For the crossover point analysis, we did not apply error adjustment (e.g., shifts or linear equations) to the measurements according to the information of gravity differences at crossover points as many researchers did before (e.g., Wessel and Watts 1988; Lequentrec-Lalancette 1992; Denker and Roland 2005; Hunegnaw et al. 2009; Lequentrec-Lalancette et al. 2016). The reason is that there is no inconsistencies in our shipborne gravimetry data due to sufficient and consistent link information. Moreover, the accuracy of shipborne gravimetry has been improved due to the development of GNSS technologies as mentioned in Sect. 2.2. On the other side, the accuracy of our shipborne gravimetry has already reached the level of sub-mGal which is much better than previous global or regional shipborne gravimetry data sets with accuracy of several or even tens of mGal. It is worth noting that the differences at crossover points would generally become smaller after some error adjustments, it does ensure that the real accuracy of shipborne gravity can be improved at all times.

Although the accuracy of shipborne gravimetry is at the sub-mGal level, there are still some special cases existing in the measurements which generally cannot be shown by the measurement differences at crossover points. Here, we use GNSS-derived kinematic vertical accelerations (1 Hz) to analyze these phenomena (seiches, squat effect) and improve the shipborne gravimetry final products. Additionally, the crucial problem of shipborne gravimetry to find a suitable cutoff wavelength (with a suitable length of the transition zone) for the FFT low-pass filter is investigated by analyzing GNSS-derived kinematic vertical accelerations and statistics

of the measurement differences at crossover points in this section. Finally, some preliminary tests in verifying the previous gravity data and improving the current geoid models are presented there.

3.1 The influence of seiches on shipborne gravimetry

One special case in shipborne gravimetry occurs in some harbors, e.g., Trelleborg, due to the influence of seiches. Based on our analyses, we find that there are still some oscillation signals in the Chekan-AM measurements (about 3 mGal) even after applying a low-pass filter with a cutoff wavelength of 400 s. In order to eliminate the residual oscillation signals, first we investigate the measurements in the frequency domain. The power spectral density (PSD) of the Chekan-AM measurements before filtering is shown in Fig. 4a. We only focus on the long-wavelength signals which are indicated by the black box. The reason is that the cutoff wavelength of the low-pass filter is generally longer than 100 s to remove the noise in the high-frequency part. From the Fig. 4b, it is seen that there are two main peaks around the wavelengths 230 s and 380 s.

In order to investigate the power strength at different wavelengths over time, we use the Continuous Wavelet Transform (CWT) analysis to study the Chekan-AM measurements in the harbor Trelleborg. Here, we use the sine-like Morlet wavelet as the mother wavelet which allows $1/s$ (s means second) to be interpreted as frequency (e.g., Grossmann and Morlet 1984; Prokoph and Barthelmes 1996). The result of the CWT analysis is shown in Fig. 4c. Some wavelength components around 230 s mainly occur at the beginning (around 8000 s) and with less power at other times while some other wavelength components around 380 s seem to exist with average power during the whole time. The mechanism of these oscillation signals is that the research vessel was inside a port basin with a rather narrow entry to the harbor (see the bottom right corner of Fig. 5) and the movements of big ferries in the same area may cause natural oscillations in the port basin, which decay only slowly. These kinds of waves are named seiches (e.g., Darwin 1898; Okihiro et al. 1993; Pinkster 2009).

In these particular cases where the measurements are affected by the seiches, we use GNSS-derived kinematic vertical accelerations to test if they can detect these signals since the research vessel is anchored in the harbor and does not move horizontally. Here, the respective measurements in the harbor Trelleborg and their PSDs are presented in Fig. 6, where Fig. 6a, b, c shows PSD of Chekan-AM measurements, PSD of GNSS-derived kinematic vertical accelerations and PSD of Chekan-AM measurements minus GNSS-derived kinematic vertical accelerations, respectively. The black, blue and brown lines in Fig. 6d represent the
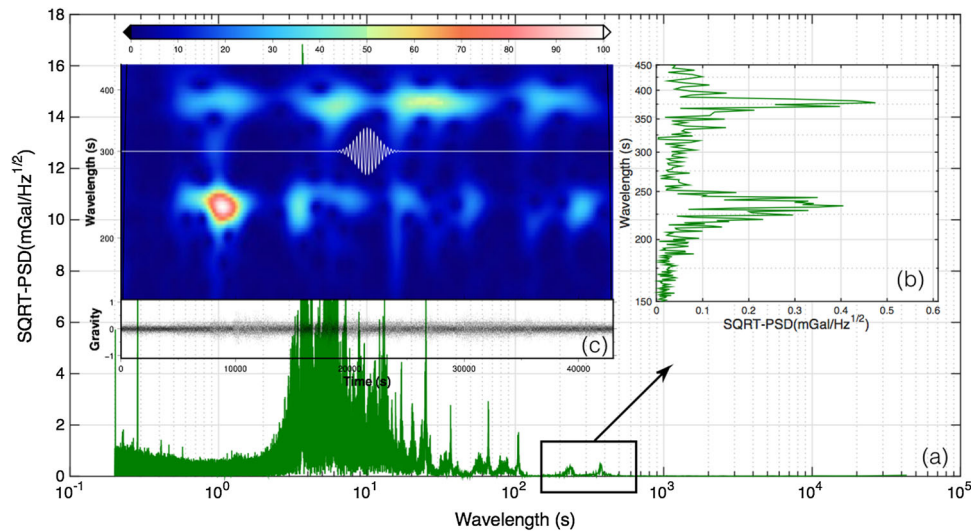
Fig. 4 a PSD of Chekan-AM measurements before filtering. **b** We are interested in the region indicated by the black box as the cutoff wavelength of the low-pass filter is regularly longer than 100 s. **c** Time–wavelength representation of normalized power (from 0 to 100) from CWT analysis shows two main wavelength components (around 230 s and 380 s). The gravity values are scaled to the interval [- 1,1] by dividing by the maximum value after removing the mean value which are also presented in the figure. The white line is one of the analyzing wavelet functions (the Morlet wavelet with the wavelength of 300 s) used in this study
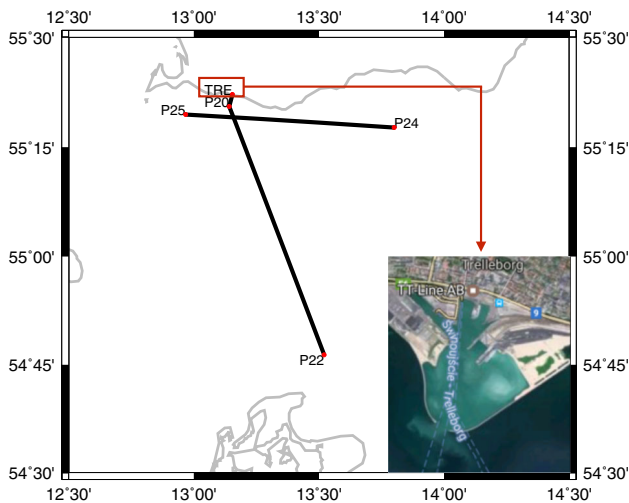

Fig. 5 Three tracks P20-TRE, P20-P22 and P24-P25 near the harbor Trelleborg. The small figure in the bottom right corner presents the structure of the harbor Trelleborg from Google Maps (Google Maps 2018)

relevant measurements in the time domain of Fig. 6a, b, c. Here, the reason of oscillation signals existing in the Chekan-AM measurements after low-pass filtering with cut-off wavelength 400 s is that there is a transition zone in the FFT low-pass filter. Moreover, some oscillation signals with the wavelength around 400 s (in the transition zone) still exist in the gravimetry measurements, although they have been suppressed. Fortunately, we find that both the gravimeter Chekan-AM and GNSS can detect these signals

which are obviously due to the vertical accelerations of the research vessel. Here, the correlation coefficient between the Chekan-AM measurements (the black line in Fig. 6d) and GNSS-derived kinematic vertical accelerations (the blue line in Fig. 6d) is - 0.96. The values of the Chekan-AM measurements after subtracting the GNSS-derived kinematic vertical accelerations are smaller than 1 mGal as seen from the brown line. It is also obvious from Fig. 6a, b, c that the PSD peaks are very consistent between Chekan-AM measurements and GNSS-derived kinematic vertical accelerations. The PSD peaks are located mainly near 400 s. After subtracting the GNSS-derived kinematic vertical accelerations from the Chekan-AM measurements, the PSD of the remaining components are much smaller compared to that of Chekan-AM measurements. In summary, GNSS-derived kinematic vertical accelerations can detect the vertical accelerations of long wavelengths due to the vertical movement of the research vessel in harbors. They can further help to separate the long-wavelength vertical acceleration signals of the research vessel from the gravity signals measured by Chekan-AM.

3.2 Determination of suitable parameters for the FFT low-pass filter

After investigating the influences of seiches on shipborne gravimetry in the harbor of Trelleborg, we analyze Chekan-AM measurements and GNSS-derived kinematic vertical accelerations for the similar long-wavelength signals in the open sea. Three example tracks P20-TRE, P20-P22 and P24-
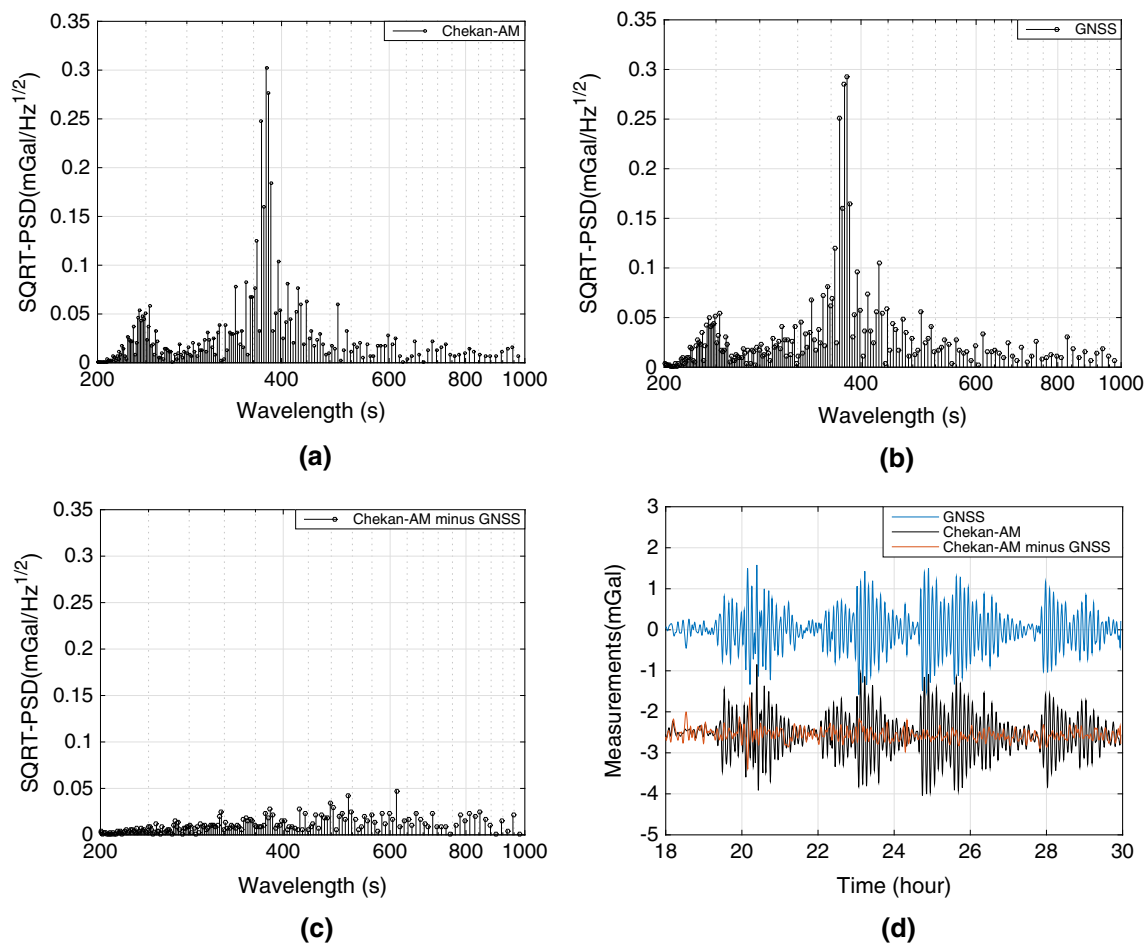
Fig. 6 Different observations in the harbor Trelleborg after low-pass filtering with cutoff wavelength 400 s: **a** PSD of Chekan-AM measurements, **b** PSD of GNSS-derived kinematic vertical accelerations, **c** PSD of Chekan-AM measurements minus GNSS-derived kinematic vertical accelerations and **d** the respective measurements. The reason of oscil-lation signals existing in the Chekan-AM measurements after low-pass filtering (with cutoff wavelength 400 s) is due to the transition zone in FFT low-pass filter. It causes some oscillation signals with wave-lengths in the transition zone leak into the measurements after filtering, although they have been suppressed

P25 near the harbor Trelleborg (see Fig. 5) are examined to check if the movements of big ferries in the sea channels have influences to the shipborne gravimetry. We choose three particular tracks to investigate, because P20-TRE is a short track (around 2.2 km) close to the harbor, P20-P22 is a track mainly in the direction of north to south (along the direction of a sea channel) and P24-P25 is a track in the direction of east to west (across sea channels). The cutoff wavelength of the FFT low-pass filter used here is 100 s which is shorter than the usual cutoff wavelength (200 s, 400 s or even longer) to help to find out the suitable cutoff wavelength for the FFT low-pass filter.

Figure 7 (a_1, b_1, c_1 and d_1) shows the results for the track P20-TRE. From the spectrum results, both the gravimeter Chekan-AM and GNSS seem to detect a signal around the wavelength of 100 s. It is for sure that the disturbing accel-erations have periods considerably longer than 6–10 s in the open Baltic Sea. Here, the correlation coefficient between the Chekan-AM measurements and GNSS-derived kinematic vertical accelerations is 0.76. One reason for the weaker cor-relation compared to that in the harbor Trelleborg is that the Chekan-AM measurements contain also the gravity signals in the track P20-TRE, although it is a very short track. Inves-tigations on the time series of the measurements show that the Chekan-AM results become smoother after subtracting the GNSS-derived kinematic vertical acceleration. Here, we use a strategy to test if the smoother measurements are still noisy: When we choose the interval of the smoother measurements to be 25 s and 50 s, the RMS of the corresponding differential series is 1.3 mGal and 1.5 mGal, respectively. As the cutoff wavelength of the FFT low-pass filter used here is 100 s, we think that the RMS of the corresponding differential series should be very small if the smoother measurements contain only gravity signals (at an accuracy level of sub-mGal). This
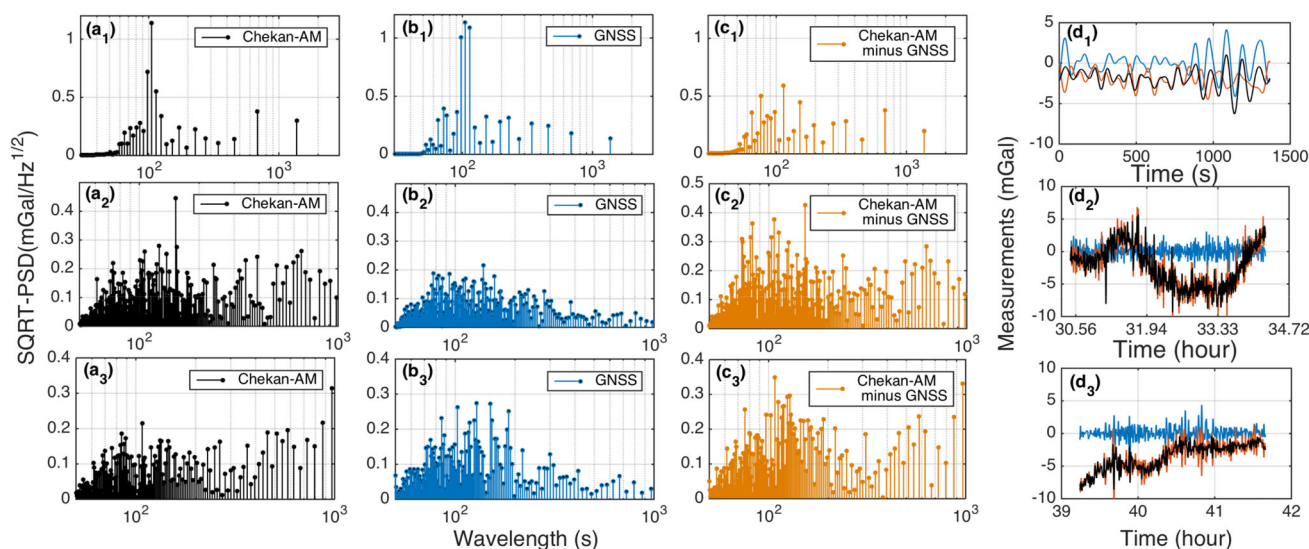
Fig. 7 Results of Track P20-TRE (a_1, b_1, c_1 and d_1), Track P20-P22 (a_2, b_2, c_2 and d_2) and P24-P25 (a_3, b_3, c_3 and d_3): ($a_{1,2,3}$) PSD of Chekan-AM measurements, ($b_{1,2,3}$) PSD of GNSS-derived kinematic vertical accelerations, ($c_{1,2,3}$) PSD of Chekan-AM measurements minus GNSS-derived kinematic vertical accelerations and ($d_{1,2,3}$) the respective measurements. The remaining signals of Chekan-AM minus GNSS are still noisy after low-pass filtering with cutoff wavelength 100 s

is another reason for the weaker correlation compared to that in the harbor Trelleborg. Therefore, we think this short track is still noisy which means that we need to apply a low-pass filter with a longer cutoff wavelength. In other words, the suitable cutoff wavelengths of the low-pass filter should be longer than 100 s.

Figure 7 (a_2, b_2, c_2 and d_2) and Fig. 7 (a_3, b_3, c_3 and d_3) present the results of the tracks P20-P22 and P24-25, respectively. They show similar results: The GNSS-derived kinematic vertical accelerations are within 5 mGal. The PSD of GNSS-derived kinematic vertical accelerations mainly concentrates between 70 and 200 s at the level of 0.2–0.3 mGal/Hz$^{1/2}$. Here, the same strategy applied to the Track P20-TRE is used: We choose the interval of 25 s and get the corresponding differential series. The RMS of the differential series from Chekan-AM measurements (alone) and that after subtracting GNSS-derived kinematic vertical accelerations are 2.0 mGal and 2.9 mGal for the track P20-22 (1.5 mGal and 2.6 mGal for the track P24-25). Although these are mobile measurements of long distance tracks, the time series and related statistics from differential series give us an impression that the Chekan-AM measurements before and after subtracting GNSS-derived kinematic vertical accelerations are both noisy. On the other hand, the correlation coefficients between the Chekan-AM measurements and GNSS-derived kinematic vertical accelerations are 0.01 and 0.03 for the tracks P20-P22 and P24-P25, respectively. One reason for such small values of the correlation coefficients is that these two tracks are very long and mainly contain the gravity signal. Therefore, the GNSS-derived kinematic vertical accelerations are

not accurate enough to separate the kinematic vertical accelerations (low PSD within 70 s and 200 s) contained in the Chekan-AM measurements. The more convincing evidence will be displayed by the statistics of gravimetry measurement differences at crossover points. Based on our tests, the values of GNSS-derived kinematic vertical accelerations becomes very small (0.3 mGal) after filtering with the cutoff wavelength of 200 s. It also cannot help to improve the Chekan-AM measurements. Therefore, a cutoff wavelength longer than 200 s may be suitable for the shipborne gravimetry. Here, the half wavelength in a spatial resolution (corresponding the cutoff wavelength of 200 s) is about 0.5 km along the tracks as the average velocity of the research vessels is about 5 m/s.

Next, to find out the most suitable cutoff wavelength and length of the transition zone, we analyze the gravity differences at crossover points (50 points) from the shipborne gravimetry mission "Deneb 2016" after FFT low-pass filtering with different parameters. Table 1 shows the RMS of gravity differences at crossover points for different cutoff wavelengths and lengths of the transition zone. From this table, the boxed cutoff wavelength (400 s) and the length of the transition zone (30% length of the cutoff wavelength) are a good set of parameters for the FFT low-pass filter considering the balance between accuracy and spatial resolution. As the average velocity of the research vessels is about 5 m/s, the half wavelength in a spatial resolution is about 1 km along the tracks. The first parameter (the cutoff wavelength) of the FFT low-pass filter is much more important than the other one (the transition zone). The differences of RMS of grav-

Table 1 RMS of absolute differences at crossover points for different cutoff wavelengths (CW) and lengths of the transition zone (LTZ). These 50 crossover points are from the shipborne gravimetry mission "Deneb 2016"

LTZ	CW						
	200 s	250 s	300 s	350 s	400 s	450 s	500 s
10%	0.80	0.83	0.88	0.73	0.53	0.54	1.37
20%	0.64	0.64	0.69	0.56	0.54	0.48	0.51
30%	0.67	0.65	0.61	0.58	0.51	0.49	0.47
30%*[a]	1.09	0.78	0.67	0.74	0.67	0.65	0.62
40%	0.65	0.62	0.62	0.59	0.56	0.56	0.51
50%	0.63	0.61	0.58	0.57	0.55	0.53	0.48

Unit: mGal. The results with "*" mean that the crossover points are from the Chekan-AM measurements after subtracting the GNSS-derived kinematic vertical accelerations

ity differences at crossover points are generally smaller than 0.05 mGal by applying the FFT low-pass filter with different transition zones (20%, 30%, 40%, and 50%) and same the cutoff wavelengths in Table 1. As mentioned in Sect. 2.3, short transition zones (e.g., 10%) are not good choices, which can be also seen from the RMS shown in the first row of the table.

To complement our investigations, we also analyze gravity differences at the crossover points from the Chekan-AM measurements after subtracting the GNSS-derived kinematic vertical accelerations. Here, the transition zone of the FFT low-pass filter is the same as the good choice without subtracting GNSS-derived kinematic vertical accelerations (see the row with "*" in Table 1). By comparing these two rows, the RMS differences between the Chekan-AM measurements (30%) and that after subtracting the GNSS-derived kine-

matic vertical accelerations (30%*) are very small (about 0.15 mGal except with the cutoff wavelength 200 s) which indicates that the vertical accelerations can be ignored after low-pass filtering with cutoff wavelengths longer than 200 s. On the other hand, the shipborne gravimetry results seem to be slightly worse after subtracting the GNSS-derived kinematic vertical accelerations after low-pass filtering, especially with the cutoff wavelengths (200 s) and the length of the transition zone (30%). Our conclusion is that the current GNSS-derived kinematic vertical accelerations are not accurate enough to separate long-wavelength kinematic vertical accelerations with small amplitudes from Chekan-AM measurements.

3.3 The influence of the squat effect on shipborne gravimetry

Two examples of the special case caused by the squat effect in shipborne gravimetry are shown in Fig. 8b: (1) and (2) are the results from one track (zP1-zP2) while (3) and (4) are from another track (zL1-zL2). Here, these two tracks are from the campaign "Capella 2013" near the German coast (see Fig. 8a). In Fig. 8b(1, 3), the blue line represents the vertical accelerations from GNSS; the magenta line represents the depth of the seafloor from bathymetry; the black line represents the Chekan-AM measurements and the brown line represents Chekan-AM measurements minus the GNSS-derived kinematic vertical accelerations, respectively. Here, the cutoff wavelength is 200 s and has been applied on GNSS as well as on Chekan-AM measurements. From the bathymetry measurements, it is obvious that the depth of the sea channel is about 11 m which is 5 m deeper than the normal seafloor of 6 m. When the research vessel crossed the
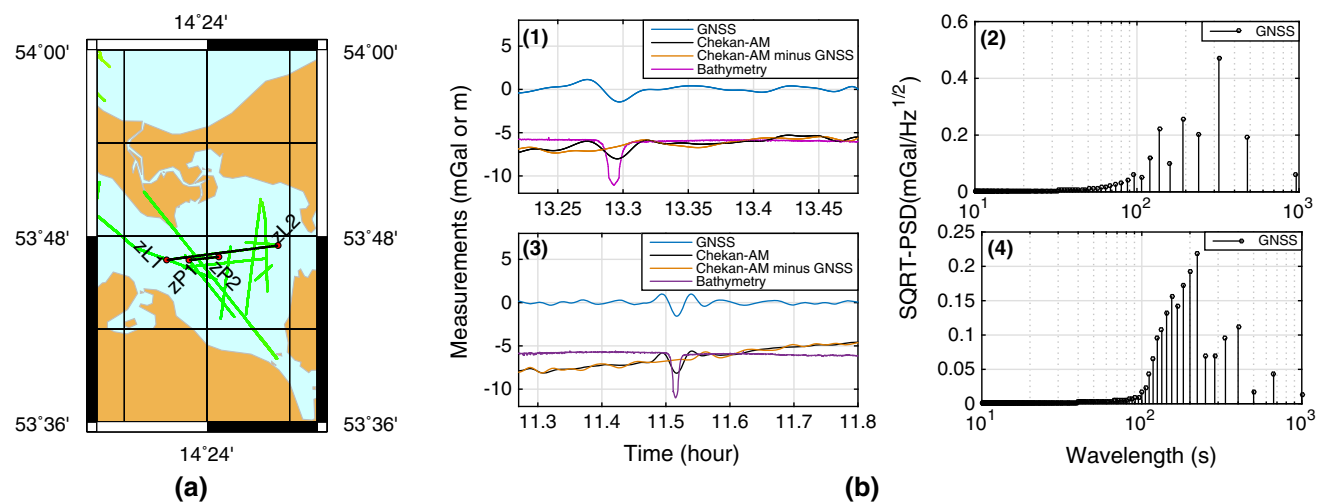

Fig. 8 **a** The positions of the tracks zP1-zP2 and zL1-zL2 crossing ship channels. **b** Gravimetry results of these two tracks: (1) and (3) different observations after low-pass filtering of these two tracks, respectively, (2) and (4) PSD for GNSS-derived kinematic vertical accelerations of these two tracks, respectively

Fig. 9 **a** The NKG gravity database in the Baltic Sea area in May 2015. Black dots are land (surface) data, red dots are either shipborne or ice measurements, blue dots are airborne and dark green sea bottom measurements (Bilker-Koivula et al. 2017). **b, c** present gravity disturbances of our shipborne gravimetry tracks in the Baltic Sea, mainly in the Gulf of Bothnia and near the coast of Germany, Poland and Sweden, respectively
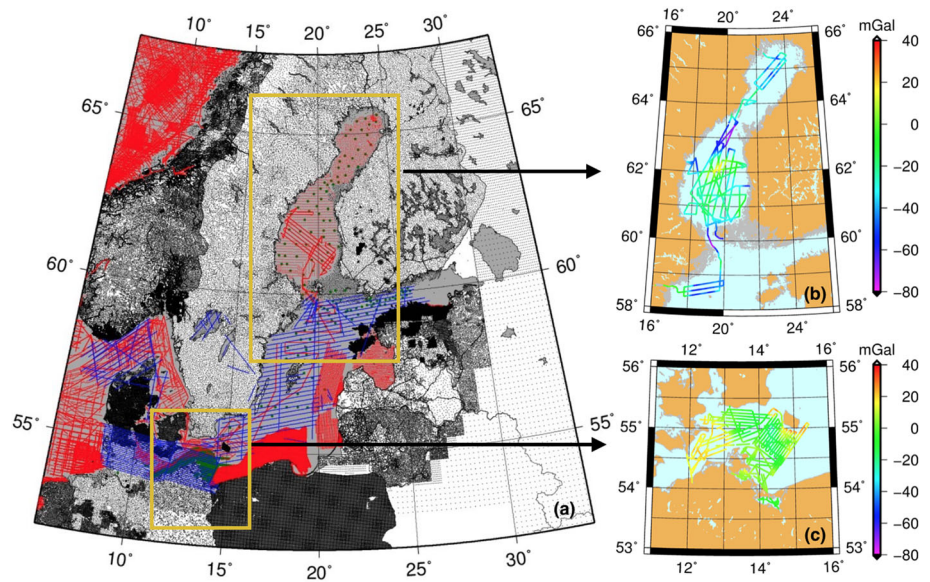
sea channel, the gravimeter Chekan-AM detected a variation of 2 mGal. This is not mainly caused by the gravitational attraction from the submarine topography effect, because the gravity (at the sea surface) over such a cuboid is about 0.3 mGal. Here, a cuboid hypothetically represents the channel with height 5 m (the depth difference between the channel and the normal seafloor), width 300 m (the width of the channel), length 1 km (or 10 km), mass–density $d\rho = 1640$ kg/m^3 (the mass–density difference between standard topographic rock and ocean water). The far topography effect is negligible for sufficiently long cuboids, i.e., 1 km and beyond. It is also not mainly caused by the gravity change due to the change of the ship elevation (sea surface height), because the maximum change of ship elevation around the channels is approximately 5 cm. Since the vertical gravity gradient is about 0.3086 mGal/m and the required accuracy of shipborne gravimetry is sub-mGal, the gravity change due to the change of the ship elevation can be ignored.

The values of GNSS-derived kinematic vertical accelerations also show similar changes of 2 mGal. Here, the correlation coefficients between the Chekan-AM measurements and GNSS-derived kinematic vertical accelerations are 0.88 and 0.91 at these channel areas of the tracks zP1-zP2 and zL1-zL2, respectively. After subtracting the GNSS-derived kinematic vertical accelerations from the Chekan-AM measurements, the variation becomes smoother or even vanishes, which further indicates that it is not gravity change but comes from the vertical accelerations of the research vessel. In other words, this phenomenon is obviously caused by the vertical movement due to the squat effect. The PSD for the GNSS-derived kinematic vertical accelerations of the tracks are shown in Fig. 8b(2, 4). It can be seen that there are signals with high amplitudes between the wavelength 100 and

1000 s, especially between 200 and 500 s. That means, a low-pass filter with the cutoff wavelength of 500 s or even longer (due to the transition zone) should be applied to Chekan-AM measurements to eliminate this phenomenon when the GNSS-derived kinematic vertical accelerations are not taken into account. However, in case of such a long cutoff wavelength, the spatial resolution of the results will be only several km which does not seem favorable for shipborne gravimetry. Fortunately, these disturbing acceleration signals can be detected by GNSS-derived kinematic vertical accelerations from the results mentioned above. With an accuracy goal of sub-mGal, the influence of the squat effect on shipborne gravimetry should be taken into account in shallow waters. It can be resolved by subtracting GNSS-derived kinematic vertical accelerations from Chekan-AM's measurements.

3.4 Preliminary tests in geoid determination

Finally, the content of the Nordic Geodetic Commission (NKG) gravity database in the Baltic Sea area and the gravity disturbances along our shipborne gravimetry tracks in the Baltic Sea are shown in Fig. 9. Two of the five shipborne gravimetry missions were done mainly in the Gulf of Bothnia, as shown in Fig. 9b. The other three shipborne gravimetry missions were done near the coast of Germany, Poland and Sweden, as shown in Fig. 9c. The range of the gravity disturbances of these tracks is from - 80 to 40 mGal. There are 380 crossover points among all these tracks. The statistical results of the gravity differences at crossover points for Minimum, Maximum, Mean, STD and RMS values are - 0.255 mGal, 2.76 mGal, 0.17 mGal, 0.74 mGal and 0.76 mGal, respectively. Therefore, the accuracy of these five shipborne gravimetry missions is $0.76/\sqrt{2} \approx 0.5$ mGal

derived from the RMS value. These tracks are mainly at such places where gravity measurements are sparse or old gravity measurements need to be verified. For example, our shipborne gravimetry results in the Gulf of Bothnia confirms that the old Håkon Mossby shipborne data of 1996 has a positive offset with respect to surrounding observations, although its size varies in the area. The impact of our shipborne gravimetry measurements on geoid determination is up to 5 cm in this area (Bilker-Koivula et al. 2017). The newer measurements on the ice from the nineties also show a similar positive offset existing in the old shipborne gravimetry data (Kaariainen and Makinen 1997).

Another preliminary test area near the cost of Germany is shown in Fig. 10. For most of the shallow German waters in the area (Greifswald Bay and about 10 km out of Ruegen and Usedom), high-resolution geophysical gravimetry data are available for geoid modeling at the BKG. Further out at sea, these are complemented by historical sea bottom measurements of the 60ies/70ies (see Fig. 9a). On the other hand, considerable data gaps existed in the adjacent areas, in particular in the northeast of the test area. The aim of the campaigns onboard the survey vessel CAPELLA in 2013 was, thus, to validate the existing data and to close data gaps. As an outcome, the older measurements could be confirmed (differences at the order of 1–2 mGal), which is an important result regarding the usability of these partly historical data sources for geoid modeling.
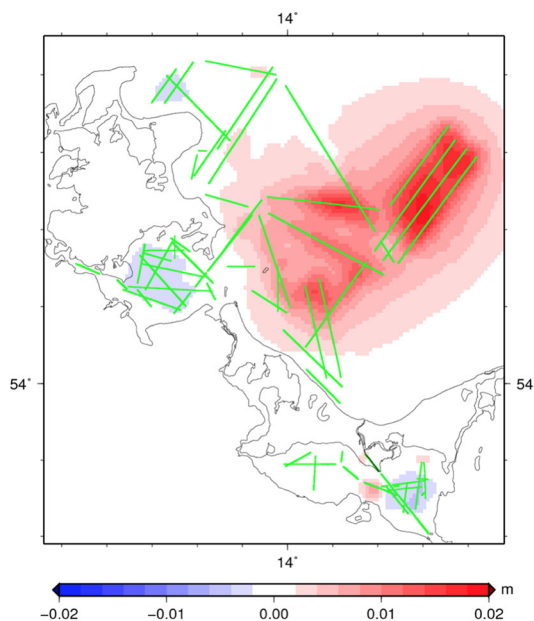
Figure 10 shows the differences between two regional geoid modeling solutions using the same data and method parameters, except for using the CAPELLA data of 2013 (green lines) or not. The modeling method used here is a remove–restore approach (the global model EIGEN-6C4 and the residual terrain modeling for reduction) in combination with a point mass adjustment of the reduced ("residual") data (Forsberg 1984; Barthelmes 1986; Förste et al. 2014; Schwabe et al. 2016). On the one hand, it can be seen that in some areas the impact of the CAPELLA data is small, i.e., limited to some millimeters. These are the areas where existing data could be confirmed. On the other hand, the largest differences (up to 2 cm) are in the northeast of the CAPELLA campaign area. This could be expected, since no real marine gravity observations are available in the adjacent Polish territories which, on the other hand, feature considerable gravity gradients in Bouguer maps. In this region, an altimetric gravity model was used as fill-in data. However, the accuracy of such data is known to be degraded in shallow coastal waters.

These preliminary geoid tests confirmed that our shipborne gravimetry data, including tie measurements at harbor points, are accurate and reliable enough to validate existing marine gravity datasets and to estimate the impact of fill-in data on the marine geoid for relevant parts of the Baltic Sea. The final aim is to calculate a high-quality geoid model for future GNSS-based navigation covering the whole Baltic Sea based on these new shipborne gravimetry measurements and old gravity measurements at this target place by 2020.

4 Discussion and Conclusions

In this article, a data processing strategy of shipborne gravimetry to get high-accurate gravity measurements with high spatial resolution in the Baltic Sea is studied. The fundamental problem to find the suitable parameters of the FFT low-pass filter is solved in two steps: first, we use GNSS-derived kinematic vertical accelerations to determine the shortest cutoff wavelength to be 200 s; Second, by investigating gravity measurement differences at crossover points, we determine the most suitable cutoff wavelength and length of the transition zone to be 400 s and 120 s (30% of the length of the cutoff wavelength), respectively. Apart from that, there are two crucial findings related to the processing of the gravimetry measurements. One is that seiches can cause oscillation signals contained in shipborne gravimetry measurements in some harbors (e.g., Trelleborg). The other one is that the squat effect can disturb shipborne gravimetry measurements in shallow water. Fortunately, we find that GNSS-derived kinematic vertical accelerations can be used for reduction of these external vertical accelerations (several mGal, at long wavelengths) remaining in the gravity measurements after low-pass filtering. However, in general, the

Fig. 10 Contribution of research vessel CAPELLA data on geoid estimation (identical processing otherwise). The green lines represent the gravimetry tracks. The differences between two regional geoid modeling solutions using the same data and method parameters, except for using the CAPELLA data or not are up to 2 cm

currently derivable GNSS-based kinematic vertical accelerations are not accurate enough to separate long-wavelength kinematic vertical accelerations with small amplitudes from Chekan-AM measurements. Finally, our RMS of gravity differences at 380 crossover points collected during the five campaigns is 0.76 mGal. This implies (according to the law of error propagation) that the accuracy for our shipborne gravimetry is $0.76/\sqrt{2} \approx 0.5$ mGal along the tracks. Some of these high-quality shipborne gravimetry measurements have been used successfully in the verification of the previous gravimetry measurements and improving geoid determination by up to 5 cm in the Baltic Sea.

References

Akaike H (1968) Low pass filter design. Ann Inst Stat Math 20(1):271–297

Barthelmes F (1986) Untersuchungen zur Approximation des äußeren Gravitationsfeldes der Erde durch Punktmassen mit optimierten Positionen. Veroffentlichungen des Zentralinstituts Physik der Erde 92

Bernoulli D (1968) Hydrodynamica (1738). Translated from Latin by T Carmody and H Kobus, Dover pub, p 128

Bilker-Koivula M, Mononen J, Saair T, Förste C, Barthelmes F, Lu B, Ågren J (2017) Improving the geoid model for future GNSS-based navigation in the Baltic Sea. In: Proceedings FIG (international federation of surveyors) working week 2017 surveying the world of tomorrow—from digitalisation to augmented reality, Helsinki, Finland

Blazhnov B (2002) Integrated mobile gravimetric system-development and test results. In: 9th Saint petersburg international conference on integrated navigation systems, St. Petersburg, pp 223–232

Bruton A, Glennie C, Schwarz K (1999) Differentiation for high-precision GPS velocity and acceleration determination. GPS Solut 2(4):7–21

Cannon ME, Lachapelle G, Szarmes MC, Hebert JM, Keith J, Jokerst S (1997) DGPS kinematic carrier phase signal simulation analysis for precise velocity and position determination. Navigation 44(2):231–245

Childers VA, Bell RE, Brozena JM (1999) Airborne gravimetry: an investigation of filtering. Geophysics 64(1):61–69

Darwin GH (1898) The tides and kindred phenomena in the solar system. Houghton Mifflin Harcourt, Boston

Denker H, Roland M (2005) Compilation and evaluation of a consistent marine gravity data set surrounding Europe. In: Sansò F (ed) A window on the future of geodesy. Springer, New York, pp 248–253

Forsberg R (1984) A study of terrain reductions, density anomalies and geophysical inversion methods in gravity field modelling. Technical report, DTIC document

Förste C, Bruinsma S, Abrikosov O, Lemoine J, Marty J, Flechtner F, Balmino G, Barthelmes F, Biancale R (2014) EIGEN-6C4 The latest combined global gravity field model including GOCE data up to degree and order 2190 of GFZ Potsdam and GRGS Toulouse. GFZ Data Services. https://doi.org/10.5880/icgem.2015.1

Google Maps (2018) The Harbor Trelleborg. https://www.google.de/maps/@55.3666474,13.1565697,2893m/data=!3m1!1e3. Accessed 12 Jul 2018

Grossmann A, Morlet J (1984) Decomposition of hardy functions into square integrable wavelets of constant shape. SIAM J Math Anal 15(4):723–736

Harlan RB (1968) Eotvos corrections for airborne gravimetry. J Geophys Res 73(14):4675–4679

Hàrting A, Reinking J, Ellmer W (2004) Ship squat in hydrography: a study of the surveying vessel Deneb. Int Hydrogr Rev 5(3):41–47

He K (2015) GNSS kinematic position and velocity determination for airborne gravimetry. Ph.D. thesis, Berlin, Technische Universität Berlin, Diss., 2014

He K, Xu T, Förste C, Petrovic S, Barthelmes F, Jiang N, Flechtner F (2016) GNSS precise kinematic positioning for multiple kinematic stations based on a priori distance constraints. Sensors 16(4):470

Hunegnaw A, Hipkin R, Edwards J (2009) A method of error adjustment for marine gravity with application to mean dynamic topography in the northern North Atlantic. J Geod 83(2):161

Jachowski J (2008) Assessment of ship squat in shallow water using CFD. Arch Civil Mech Eng 8(1):27–36

Jekeli C (2001) Inertial navigation systems with geodetic applications. Walter de Gruyter, Berlin

Kaariainen J, Makinen J (1997) The 1979–1996 gravity survey and results of the gravity survey of Finland 1945–1996 NASA (19980024670)

Krasnov A, Sokolov A (2015) A modern software system of a mobile Chekan-AM gravimeter. Gyroscopy Navig 6(4):278–287

Krasnov A, Sokolov A, Usov S (2011) Modern equipment and methods for gravity investigation in hard-to-reach regions. Gyroscopy Navig 2(3):178–183

Krasnov A, Sokolov A, Elinson L (2014) Operational experience with the Chekan-AM gravimeters. Gyroscopy Navig 5(3):181–185

Lequentrec-Lalancette MF (1992) Les sources d'erreur en gravimétrie marine. Rapport Technique Didacticiel du BGI

Lequentrec-Lalancette M, Salaün C, Bonvalot S, Rouxel D, Bruinsma S (2016) Exploitation of marine gravity measurements of the mediterranean in the validation of global gravity field models. In: International symposium on earth and environmental sciences for future generations. Springer, pp 63–67

Li M, He K, Xu T, Lu B (2018) Robust adaptive filter for shipborne kinematic positioning and velocity determination during the Baltic Sea experiment. GPS Solut 22(3):81

Lu B, Barthelmes F, Petrovic S, Förste C, Flechtner F, Luo Z, He K, Li M (2017) Airborne gravimetry of GEOHALO mission: data processing and gravity field modeling. J Geophys Res Solid Earth. https://doi.org/10.1002/2017JB014425

Okihiro M, Guza R, Seymour R (1993) Excitation of seiche observed in a small harbor. J Geophys Res Oceans 98(C10):18201–18211

Petrovic S, Barthelmes F, Pflug H (2016) Airborne and shipborne gravimetry at GFZ with emphasis on the GEOHALO project. In: Rizos C, Willis P (eds) IAG 150 years: proceedings of the 2013 IAG scientific assembly, Potsdam, Germany, 2013. Springer, pp 313–322. https://doi.org/10.1007/1345_2015_17

Pinkster J (2009) Suction, seiche, and wash effects of passing ships in ports. Trans Soc Naval Archit Mar Eng 117:99

Prokoph A, Barthelmes F (1996) Detection of nonstationarities in geological time series: wavelet transform of chaotic and cyclic sequences. Comput Geosci 22(10):1097–1108

Rabiner LR, Gold B (1975) Theory and application of digital signal processing. Prentice-Hall Inc, Englewood Cliffs, p 777

Schwabe J, Liebsch G, Schirmer U (2016) Refined computation strategies for the new German combined quasigeoid GCG2016. In: Proceedings the "international symposium on gravity, geoid and height systems 2016 (GGHS 2016), Thessaloniki, Greece

Serrano L, Kim D, Langley RB (2004) A single GPS receiver as a real-time, accurate velocity and acceleration sensor. In: Proceedings of the the 17th international technical meeting of the satellite division of the institute of navigation (ION GNSS 2004), Long Beach, CA, USA, vol 2124

Sokolov A (2011) High accuracy airborne gravity measurements. Methods and equipment. In: IFAC proceedings volumes (IFAC-PapersOnline), proceedings 18th IFAC world congress, pp 1889–1891

Varyani K (2006) Squat effects on high speed craft in restricted waterways. Ocean Eng 33(3):365–381

Wessel P, Watts AB (1988) On the accuracy of marine gravity measurements. J Geophys Res Solid Earth 93(B1):393–413

Zheleznyak L (2010) The accuracy of measurements by the CHEKAN-AM gravity system at sea. Izv Phys Solid Earth 46(11):1000–1003

Zheleznyak L, Koneshov V, Krasnov A, Sokolov A, Elinson L (2015) The results of testing the Chekan gravimeter at the Leningrad gravimetric testing area. Izv Phys Solid Earth 51(2):315–320